

## Hexagonal to Cubic Phase Transition in the D<sub>2</sub>O-Induced Reverse Micellar Solution of a PEO-*b*-PPO-*b*-PEO Block Copolymer

Do Hyun Kim, Yoon Soo Ko, and Yong Ku Kwon\*

Department of Polymer Science and Engineering, Inha University, Incheon 402-751, Korea

Received September 9, 2007; Revised January 12, 2008

**Abstract:** The morphology of the D<sub>2</sub>O-induced reverse micellar structure of an amphiphilic block copolymer of poly(ethylene oxide)-*b*-poly(propylene oxide)-*b*-poly(ethylene oxide)(EO<sub>76</sub>PO<sub>29</sub>EO<sub>76</sub>) was investigated in hydrophobic media by small angle neutron scattering (SANS). Increasing D<sub>2</sub>O in the styrene/divinylbenzene solution of EO<sub>76</sub>PO<sub>29</sub>EO<sub>76</sub> led to a change in morphology of the reverse micelles from a short range ordered molecular aggregate to a hexagonally arranged micelle, and further to a spherical micelle.

**Keywords:** reverse micelles, amphiphilic block copolymer, small angle neutron scattering.

### Introduction

Recent research effort has focused on developing nanoporous materials with various framework compositions in an attempt to expand the range of materials available for the applications in many practical uses.<sup>1-3</sup> Nanoporous materials with an organically modified or organic framework are potentially useful in the separation,<sup>4</sup> purification,<sup>5,6</sup> trace adsorption<sup>7</sup> and stereoselective synthesis.<sup>8</sup> It is known that they can be prepared by several synthetic pathways including controlled foaming,<sup>9,10</sup> ion track etching,<sup>11</sup> and molecular imprinting<sup>12</sup> and so on. Typical synthesis has been carried out by polymerizing organic monomers in the presence of ionic surfactants<sup>13</sup> or non-ionic amphiphilic block copolymers<sup>14,15</sup> as a structure-directing templating material. Since the interaction between monomers and amphiphiles was assumed to be almost absent, a long-range nanoscopic order of pore structure was unaffected during the polymerization of monomers in the framework phase.<sup>16</sup>

Non-ionic block copolymers as a templating material are effective to control pore geometry such as diameter and thickness.<sup>17</sup> They also form a polymolecular micelle in the presence of oil or water in aqueous or hydrophobic organic solvent media. In the synthesis of inorganic mesoporous silica, hydrophobic swelling agent, for example, 1,3,5-trimethylbenzene (TMB) was often added to control the pore diameter by preferential solubilization in the micelle.<sup>18,19</sup> When TMB is added to the aqueous solution of a symmetric non-ionic surfactant, poly(ethylene oxide)-*b*-poly(propylene oxide)-*b*-poly(ethylene oxide) with the molar ratios of eth-

ylene oxide (EO) at both ends and propylene oxide (PO) of 20 and 70, respectively (EO<sub>20</sub>PO<sub>70</sub>EO<sub>20</sub>), a hexagonal nanoscopic ordering of micelles could be only observed at molar ratios of TMB/EO<sub>20</sub>PO<sub>70</sub>EO<sub>20</sub> less than 0.2-0.3.<sup>20</sup> With further increasing TMB in the mixture, a transition from a hexagonal cylindrical phase to a spherical mesocellular silica phase was observed. In hydrophobic media, the micellar property of non-ionic block copolymers was controlled by varying the molar ratio of water to hydrophilic block segment such as EO. It reported that EO<sub>8</sub>PO<sub>50</sub>EO<sub>8</sub> did not form a polymolecular micelle when the molar ratio (*w*) of water/EO < 0.35. Spherical micelles were formed for *w* < 1.3 and became nonspherical for *w* > 1.3.<sup>21</sup>

In the present study, we prepare a D<sub>2</sub>O induced the reverse micellar structure of an amphiphilic block copolymer of EO<sub>76</sub>PO<sub>29</sub>EO<sub>76</sub> in hydrophobic media. To explore the effect of D<sub>2</sub>O on the phase morphology of block copolymer micelles, small angle neutron scattering (SANS) technique is employed at various molar ratios of D<sub>2</sub>O/block copolymer in the mixture of styrene (St) and divinylbenzene (DVB), which may be cured during further treatments to form a crosslinked polymeric resin. Since the specific interaction between monomers and EO<sub>76</sub>PO<sub>29</sub>EO<sub>76</sub> is almost absent in our system and the morphology of the crosslinked polymeric resins is therefore almost the same as that of block copolymer micelles in St/DVB solution, the data obtained from this study will provide the valuable information on the morphology of the final cured polymeric resins.

### Experimental

A triblock copolymer EO<sub>76</sub>PO<sub>29</sub>EO<sub>76</sub> (number average

\*Corresponding Author. E-mail: ykkwon@inha.ac.kr

molecular weight of  $M_n = 8,400$  g/mol) was purchased from Aldrich and used as received. Styrene and divinylbenzene were purchased from Aldrich and washed with aqueous NaOH (25 wt%) and distilled water for several times for removal of inhibitor and any residual reagent. Then they were dried with anhydrous magnesium sulfate prior to use. 2,2'-Azobisisobutyronitrile (AIBN) was purchased from Aldrich and recrystallized prior to use.

SANS experiments were carried out on the facility at the HANARO center in KAERI in Korea with a two dimensional position sensitive  $65 \times 65$  cm<sup>2</sup> detector. The equipment employs a circular pinhole collimation with Bi/Be filter. The neutron scattering intensity was measured using a neutron wavelength of 5.08 Å with wavelength resolution  $\Delta\lambda/\lambda \sim 11.8\%$  at the sample-to-detector distance of 3 m, covering a  $Q$  ( $4\pi \sin\theta/\lambda$  where  $2\theta$  is scattering angle) range of 0.01-0.24 Å<sup>-1</sup>. A quartz cell with 2 mm path length was used as a sample container and samples were loaded at room temperature. The scattered intensities were converted to an absolute differential scattering cross section per unit sample volume after calibration with a silica standard (NIST). The data have been multiplied by a factor of  $\sim 10^1$  to  $10^{1.5}$  to avoid overlapping between data. The backgrounds from the St/DVB mixture and quartz cell were also subtracted. To prepare the specimens for SANS measurement, triblock copolymers were dissolved and stirred vigorously in the mixtures of St and DVB (volume fraction of St of 60%) for several hours. The concentration of block polymers was fixed at 20 wt%.

## Results and Discussion

To induce the polymolecular reverse micellar formation of EO<sub>76</sub>PO<sub>29</sub>EO<sub>76</sub>, the calculated amount of D<sub>2</sub>O was added. The molar ratio ( $w$ ) between D<sub>2</sub>O and EO segment varied from 0 to 2.3 to investigate the change in the reverse micellar morphology of EO<sub>76</sub>PO<sub>29</sub>EO<sub>76</sub> in the St/DVB mixed solution. Figures 1 and 2 show 2- and 1-dimensional SANS data obtained from the reaction mixtures of EO<sub>76</sub>PO<sub>29</sub>EO<sub>76</sub>/St/DVB/D<sub>2</sub>O with various molar ratios of D<sub>2</sub>O/EO. In our SANS measurement, the scattered intensity of the mixed solution only exhibited a gradual decay in the range of  $0.01 \leq Q$  (Å<sup>-1</sup>)  $\leq 0.23$  without the addition of D<sub>2</sub>O ( $w = 0$ ). As  $w$  increased from 0 to near 0.1 or 0.15, an extremely weak peak began to appear at  $Q \sim 0.033$  Å<sup>-1</sup>. With increasing the D<sub>2</sub>O content from  $w = 0.15$  in the mixture, a major intense peak appeared in the range of  $0.016 \leq Q$  (Å<sup>-1</sup>)  $\leq 0.025$ , together with a series of weak high order peaks at higher  $Q$  values (Figure 2). The presence of the strong SANS peaks for  $w \geq 0.20$  clearly indicated the formation of a two-dimensional reverse micellar ordering of EO<sub>76</sub>PO<sub>29</sub>EO<sub>76</sub> by D<sub>2</sub>O in St/DVB. The broadness of the observed peaks was due to the short-range order of the reverse micellar structure, as well as the absence of monochromator in the SANS apparatus used in

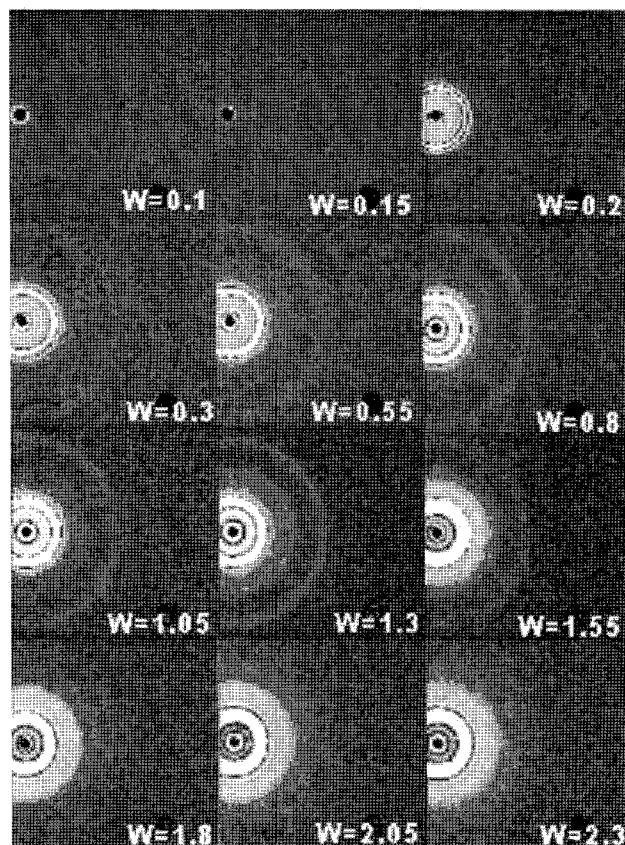


Figure 1. 2-Dimensional SANS data of the reaction mixtures of EO<sub>76</sub>PO<sub>29</sub>EO<sub>76</sub>/St/DVB/D<sub>2</sub>O with various D<sub>2</sub>O/EO ratios.

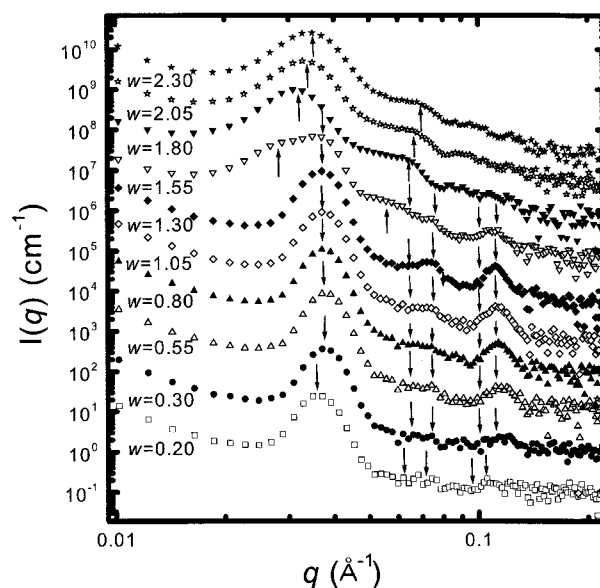


Figure 2. 1-Dimensional SANS scan data of the reaction mixtures of EO<sub>76</sub>PO<sub>29</sub>EO<sub>76</sub>/St/DVB/D<sub>2</sub>O with various D<sub>2</sub>O/EO ratios.

the present study. The major intense peaks from the mixtures with  $0.30 \leq w \leq 1.30$  were observed at  $Q \sim 0.036$  Å<sup>-1</sup> and the corresponding additional higher order peaks were observed

at  $Q$ s which were approximately in the ratio of  $\sqrt{3}$ , 2,  $\sqrt{7}$ , indicating a hexagonal packing of  $\text{EO}_{76}\text{PO}_{29}\text{EO}_{76}$  columnar micelles. Based on the positions of the major peaks, the lattice parameters were estimated as  $a = b = 202 \pm 9 \text{ \AA}$ . With these values, the calculated positions of the high order peaks were also marked as downward arrows in Figure 2.

The absence of the reverse micellar ordering for  $w = 0$  and the appearance of the extremely weak peak as  $w$  increases to  $0.1 \sim 0.15$  implied that  $\text{D}_2\text{O}$  played a significant role to induce a polymolecular reverse micellar ordering of  $\text{EO}_{76}\text{PO}_{29}\text{EO}_{76}$  in St/DVB. However, the weakness of the peak intensity for  $w = 0.1$  and  $0.15$  indicated that the molecular association of  $\text{EO}_{76}\text{PO}_{29}\text{EO}_{76}$  by  $\text{D}_2\text{O}$  was not globally occurred in St/DVB. However, the fact that the position of this weak peak was almost the same as that of the major intense peak for  $0.30 \leq w \leq 1.30$  pointed out that the approximate micellar size or the aggregation number of  $\text{EO}_{76}\text{PO}_{29}\text{EO}_{76}$  in a micelle for  $0 < w \leq 0.15$  was almost the same as that measured for  $0.20 \leq w \leq 1.30$ . A slight increase of the peak intensity and sharpness without a change in peak position as the  $w$  increases from  $0.30$  to  $1.30$  indicated that the addition of  $\text{D}_2\text{O}$  in this  $w$  range did not increase the size of the reverse micelle, but its population in the mixture.

The positions of the observed SANS peaks for  $0.30 \leq w \leq 1.30$  were almost the same, indicating that the morphology of the micellar structure was not greatly changed. With increasing  $w$  from  $0.20$  to  $0.30$ , the position of the major peak was slightly shifted to the wide-angle region. This may be due to a closer contact or packing between the  $\text{EO}_{76}\text{PO}_{29}\text{EO}_{76}$  columnar micelles at  $w = 0.30$ . Near this concentration regime, called critical gel concentration (CGC), these micelles are overlapped and ordered. By visual inspection, the mixture solutions became viscous near  $w = 0.30$ . On further addition of  $\text{D}_2\text{O}$  up to  $w \sim 1.30$  from  $0.30$ , the improvement in the packing order of the micelles resulted in the better peak profile especially at higher  $Q$  values.

On further increase of  $\text{D}_2\text{O}$  to  $w = 1.55$ , the major peak became broader and an additional weak peak intensity was found at  $Q = 0.029 \pm 0.003 \text{ \AA}^{-1}$  on its left shoulder. As  $\text{D}_2\text{O}$  further increases from  $w = 1.80$  to  $2.30$ , the peak profile was clearly different from those observed for  $w < 1.55$ . These results revealed that the preexisting hexagonal columnar phase was converted into a disordered spherical micellar phase. The broadness of the peaks for  $1.80 \leq w \leq 2.30$  was due to the liquid nature of the micellar structure which caused the spatial distribution of the scattering center of the micelle. The diameters of the spherical phase [ $d = 1.23(2\pi/Q)$ ]<sup>11</sup> were estimated as  $266 \pm 9$ ,  $263 \pm 8$ ,  $257 \pm 8 \text{ \AA}$  for  $w = 1.80$ ,  $2.05$ , and  $2.30$ , respectively. In this phase, the part of  $\text{D}_2\text{O}$  may associate with the hydrophilic EO block in the core or locate near the center of the micelle as free  $\text{D}_2\text{O}$ . The hydrophobic PO blocks are preferentially located in the surface region of the micelle as shown in Figure 3. The calculated positions of the peaks due to the spherical phase

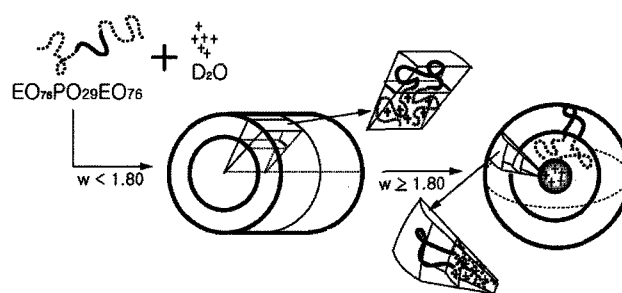


**Figure 3.** Schematic representation for the columnar and spherical micelles of the  $\text{EO}_{76}\text{PO}_{29}\text{EO}_{76}/\text{D}_2\text{O}$  mixture in St/DVB.

were marked as upward arrows in Figure 2.

Other block copolymers  $\text{EO}_{15}\text{PO}_{53}\text{EO}_{15}$  and  $\text{EO}_{20}\text{PO}_{70}\text{EO}_{20}$  were also used in our study to prepare reverse micellar solutions with  $\text{D}_2\text{O}$  in hydrophobic media, but a strong SANS peak was not detected in the similar  $Q$  range. The absence of a nanoscopic ordering for these block polymers was probably due to the short hydrophilic EO blocks at both ends which could not be strongly anchored within the core of the micelles.

## Conclusions

The effect of  $\text{D}_2\text{O}$  in the mixture of  $\text{EO}_{76}\text{PO}_{29}\text{EO}_{76}/\text{St}/\text{DVB}/\text{D}_2\text{O}$  on the formation of the reverse micelles of  $\text{EO}_{76}\text{PO}_{29}\text{EO}_{76}$  in hydrophobic St/DVB media was explored by SANS technique.  $\text{D}_2\text{O}$  played a significant role of the formation of the reverse micellar ordering of  $\text{EO}_{76}\text{PO}_{29}\text{EO}_{76}$ . The variation in the amount of  $\text{D}_2\text{O}$  successfully controlled the reverse micellar morphology of  $\text{EO}_{76}\text{PO}_{29}\text{EO}_{76}$ . Increasing the amount of  $\text{D}_2\text{O}$  in the mixture led to a change in morphology from a disordered state to a hexagonal columnar structure, which further changed into a disordered, spherical mesocellular phase. Assuming the morphology of the crosslinked polymeric resins is almost the same as that of block copolymer micelles in St/DVB solution, the data obtained from the present study provide the valuable information on the morphology of the cured polymeric resins.

**Acknowledgments.** The authors acknowledge Drs. Jeong-Soo Lee and Ki-Yeon Kim in KAERI for their assistance on our SANS measurement. Funding for this work was provided by Inha University Research Grant.

## References

- (1) A. Corma, M. T. Navarro, and J. Pérez-Pariante, *Chem. Commun.*, 147 (1994).
- (2) H. Kosslick, G. Lischke, G. Walther, W. Storek, A. Martin, and R. Fricke, *Microporous Mater.*, **9**, 13 (1997).
- (3) O. N. Le and R. T. Thomson, U.S. Patent 5 232 580 (1993).
- (4) B. Sellergren, M. Lepisto, and K. Mosbach, *J. Am. Chem.*

- Soc.*, **110**, 5853 (1988).
- (5) F. H. Arnold, P. Dhah, D. Shnec, and S. Plunkett, U.S. Patent 91-649470 (1992).
- (6) K. Dabulis and A. M. Klibanov, *Biotechnol. Bioeng.*, **39**, 176 (1992).
- (7) G. Viatakis, L. I. Andersson, R. Mueller, and K. Mosbach, *Nature*, **361**, 645 (1993).
- (8) J. Damen and D. C. Neckers, *J. Am. Chem. Soc.*, **102**, 3265 (1980).
- (9) B. Krause, H. J. P. Sijbesma, P. Munuklu, N. F. A. van der Vegt, and M. Wessling, *Macromolecules*, **34**, 8792 (2001).
- (10) B. Krause, K. Diekmann, N. F. A. van der Vegt, and M. Wessling, *Macromolecules*, **35**, 1738 (2002).
- (11) C. R. Martin, *Chem. Mater.*, **8**, 1739 (1996).
- (12) G. Wulff, *Chem. Rev.*, **102**, 1 (2002).
- (13) L. R. Dai, T. W. Wang, L. T. Bu, and G. Chen, *Colloid Surface A*, **181**, 151 (2001).
- (14) K. Mortensen, *Colloid Surface A*, **183-185**, 277 (2001).
- (15) K.-W. Kwon, M. J. Park, J. Hwang, and K. H. Char, *Polym. J.*, **33**, 404 (2001).
- (16) P. M. Lipic, F. S. Bates, and M. A. Hillmyer, *J. Am. Chem. Soc.*, **120**, 8963 (1998).
- (17) D. Zhao, J. Feng, Q. Huo, N. Melosh, G. H. Fredrickson, B. F. Chmelka, and G. D. Stucky, *Science*, **279**, 548 (1998).
- (18) C. T. Kresge, M. E. Leonowicz, W. J. Roth, J. C. Vartuli, and J. S. Beck, *Nature*, **359**, 710 (1992).
- (19) J. S. Beck, J. C. Vartuli, W. J. Roth, and M. E. Leonowicz, *J. Am. Chem. Soc.*, **114**, 10834 (1992).
- (20) J. S. Lettow, Y. J. Han, P. Schmidt-Winkel, P. Yang, D. Zhao, G. D. Stucky, and J. Y. Ying, *Langmuir*, **16**, 8291 (2000).
- (21) C. Guo, H.-Z. Liu, and J.-Y. Chen, *Colloid Surface A*, **175**, 193 (2000).